Bioconjugate Chemistry

Article

pubs.acs.org/bc

Magnetic Norbornene Polymer as Multiresponsive Nanocarrier for Site Specific Cancer Therapy

Vijayakameswara Rao N,[†] Mutyala Naidu Ganivada,[†] Santu Sarkar,[†] Himadri Dinda,[†] Koushik Chatterjee,[†] Tanmoy Dalui,[‡] Jayasri Das Sarma,[‡] and Raja Shunmugam*[,†]

[†]Polymer Research Centre, Department of Chemical Sciences, [‡]Department of Biological Sciences, Indian Institute of Science Education and Research Kolkata, BCKV main campus, Mohanpur P.O., Mohanpur, West Bengal, India 741252

Supporting Information

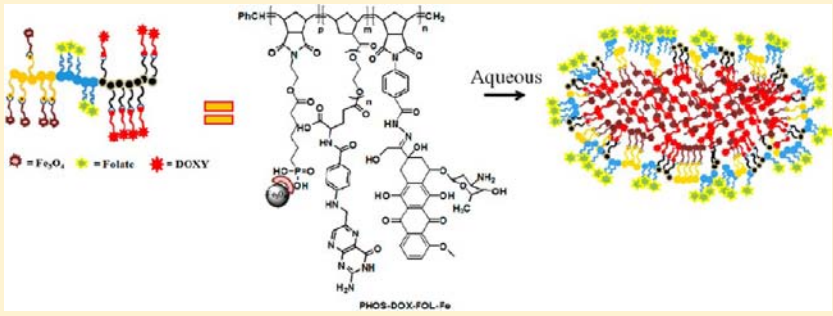

ABSTRACT: A site-specific, stimuli-responsive nanocarrier has been synthesized by conjugating folate, magnetic particles and doxorubicin to the backbone of norbornene polymer. Monomers, namely, cis-5-norbornene-6-(diethoxyphosphoryl)hexanote (**mono 1**), norbornene grafted poly(ethyleneglycol)-folate (**mono 2**), and norbornene derived doxorubicin (**mono 3**) are carefully designed to demonstrate the smart nanorcarrier capabilities. The synthesis and complete characterization of all three monomers are elaborately discussed. Their copolymerization is done by controlled/living ring-opening metathesis polymerization (ROMP) to get the triblock copolymer **PHOS-FOL-DOX**. NMR spectroscopy and gel permeation chromatography confirm the formation of the triblock copolymer, while FT-IR spectroscopy, thermogravimetric analysis, along with transmission electron microscope confirm the anchoring of iron particle (Fe_3O_4) to the **PHOS-FOL-DOX**. Drug release profile shows the importance of having the hydrazone linker that helps to release the drug exactly at the mild acidic conditions resembling the pH of the cancerous cells. The newly designed nanocarrier shows greater internalization (about 8 times) due to magnetic field. Also, increased intracellular **DOX** release is observed due to the folate receptor. From these results, it is clear that **PHOS-FOL-DOX** has the potential to act as a smart nanoreservoir with the magnetic field guidance, folate receptor targeting, and finally pH stimulation.

INTRODUCTION

The lack of efficacious therapy with minimal toxicity remains the major issue in cancer treatment.[1,2] The existing strategy to achieve active tumor targeting is to label the micelle with specific ligands that can interact with the cancer cell surface.[3] Folic acid (**FOL**) is one of the well-known targeting ligands, since the cancer cell surface is overexpressed with folate receptors.[4] However, for the selective recognition to happen between the nanocarrier and the cancer cell surface, the nanocarrier should first reach the tumor sites without losing its activity.[5,6] For improving drug delivery efficiency, an external targeting strategy is followed where a guided magnetic field holds the micelles in and effectively drives them into tumor tissues.[7,8]

Recently, efforts have been focused on developing drugs through self-assembly or high-throughput processes to facilitate the development. Drugs covalently bound in polymeric micellar cores via pH-sensitive linkers such as an imine,[9] acetal,[10] oxime,[11] or orthoester[12] have shown an enhanced in vitro cytotoxicity compared to free drug formed by rapid release of drug from acidic endosomes. Hydrazone linkers are specifically interesting for their responsive acuteness in delivery behavior.[13] Thus, we envisioned that if we conjugate the magnetic nanoparticles (Fe_3O_4) into the polymer backbone along with doxorubicin and folic acid motifs, the resulting pH-responsive amphiphilic polymers would form a nanocarrier for cancer therapy.

To produce the proposed nanocarriers, we have utilized ROMP technique,[14−17] the living ring-opening metathesis polymerization (**ROMP**) which is very attractive for synthesizing monodisperse polymeric prodrugs due to the exceptional functional group tolerance of the Grubbs' catalyst.[18−20]

Herein, we report an efficient method to prepare a stimuli responsive smart nanocarrier for controlled doxorubicin drug delivery and MRI imaging. All the three functionalities, namely, phosphonate ester (**PHO**), folic acid (**FOL**), and doxorubicin

Received: September 5, 2013
Revised: December 20, 2013
Published: December 21, 2013

   dx.doi.org/10.1021/bc400409n | *Bioconjugate Chem.* 2014, 25, 276−285

Scheme 1. Synthesis of PHO-FOL-DOX

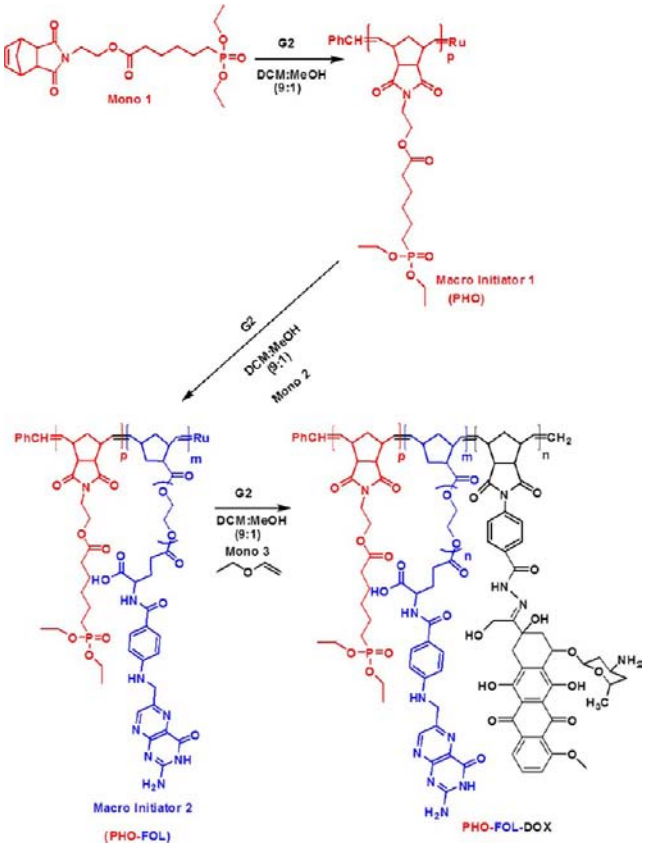

(**DOX**) are delicately conjugated to the norbornene backbone to produce novel monomers. ROMP of these monomers has produced well-defined block copolymerization to get the triblock copolymer (**PHO-FOL-DOX**) with excellent control in polydispersity index (PDI). We believe that the resulting unique nanocarrier of **PHOS-FOL-DOX-Fe** copolymer has several advantages as follows. First, the system demonstrates uniqueness by conjugating the drug as well as target ligands to the polymer backbone. This is entirely in contrast to the existing literature examples that show the encapsulation technique where they encapsulate either drug or targeting ligands such as magnetic particles and **FOL**. Second, the amount of drug, NPs, and **FOL** can be precisely controlled as per the requirement. This is achieved because of the controlled polymerization of norbornene monomers that have been conjugated with drug and targeting ligands. Third, the drug delivery process could be easily guided by magnetic field due to the magnetic NPs conjugated in the nanocarriers. In addition, the presence of FOL motif will be effectively received at the surface of the cancer cell due to the overexpressed folate receptor. To best of our knowledge, this is the efficient method that elegantly synthesizes a triblock copolymer using ROMP technique to produce a smart nanocarrier that has potential in muti-stimuli-responsive cancer therapy.

EXPERIMENTAL SECTION

Synthesis of Triblock Copolymer (PHO-FOL-DOX). Known amounts of monomers, **mono 1**, **2**, and **3** were weighed into three separate Schlenk flasks, placed under an atmosphere of nitrogen, and dissolved in anhydrous dichloromethane and methanol (9:1 v/v %). Into another Schlenk flask, 3.2 mg (15 mol %) of second generation Grubbs' catalyst was added, flushed with nitrogen, and dissolved in a minimum amount of anhydrous dichloromethane and methanol (9:1 v/v %). All three flasks were degassed three times by freeze−pump−thaw cycles. **Mono 1** (25 mg) was transferred to the flask containing the catalyst via a cannula. The reaction was allowed to stir at room temperature until the polymerization was complete (2 h); an

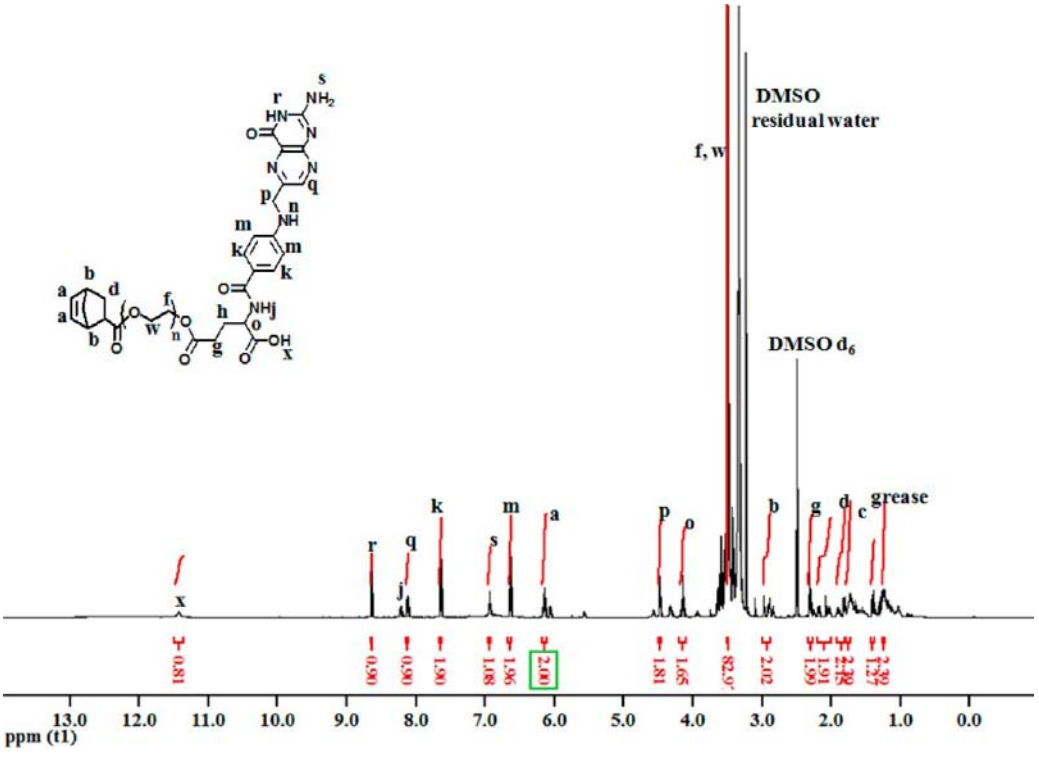

Figure 1. ^{1}H NMR spectrum of **mono 2**.

dx.doi.org/10.1021/bc400409n | *Bioconjugate Chem.* 2014, 25, 276−285

aliquot sample was taken for GPC analysis. Gel permeation chromatography was done in tetrahydrofuran (flow rate = 1 mL/min). The molecular weight of the macro initiator **1** (**PHO**) was measured as Mn = 4000, using polystyrene standards. Then the second **mono 2** (65.8 mg) was added to the flask via a cannula. The polymerization was allowed to continue for another 8 h until the polymerization was complete. An aliquot of the sample was taken for GPC analysis. The molecular weight of the macro initiator **2** (**PHO-FOL**) was measured as Mn = 17 000 using polystyrene standards. Finally, **mono 3** (46.5 mg) was added to the flask via a cannula. The reaction was allowed to stir at room temperature until the polymerization was complete. Then the reaction mixture was quenched with ethyl vinyl ether (0.5 mL). An aliquot was taken for GPC analysis, and the remaining product was precipitated from pentane, dissolved again in THF, passed through neutral alumina to remove the catalyst, and precipitated again from pentane to get a pure **PHO-FOL-DOX**. The molecular weight of the final triblock was measured as Mn = 33 000, PDI = 1.05 (Figure 2b). ^{1}H NMR (DMSO-d_6, 500 MHz): Figure 2c. IR (KBr, cm^{-1}): 3425, 2928, 2853, 1704, 1627, 1576, 1395, 1242, 1187, 1025, 964.

Deprotection of Phosphonate Ester in Triblock Copolymer (PHOS-FOL-DOX). Deprotection of phosphonate ester was carried out as mentioned in the literature. Trimethylsilyl bromide (9.8 mL, 7.5 × 10^{-2} mmol) was added slowly to a solution of **PHO-FOL-DOX** (25 mg, 7.5 × 10^{-4} mmol) in 8 mL of dry dichloromethane. After stirring under room temperature for 12 h, excess trimethylsilyl bromide and the solvent were removed under reduced pressure. Twenty milliliters of methanol/CH_2Cl_2 (3:1 v/v) mixture was added and stirred for 15 h at room temperature. Finally, the excess solvent was evaporated, and the polymer was purified by addition of excess diethyl ether. In the process, 20 mg (60% yields) of red color polymer was obtained. ^{1}H NMR (DMSO-d_6, 500 MHz): Figure 2d. IR (KBr, cm^{-1}): 3366, 2926, 2854, 1643, 1578, 1448, 1219, 1019, 772 (SI Figure S18b).

Fe_3O_4 particle attachment to PHOS-FOL-DOX to prepare PHOS-FOL-DOX-Fe. Magnetic nanoparticles were prepared by following the literature procedure. Freshly synthesized Fe_3O_4 nanoparticles were functionalized with the **PHOS-FOL-DOX** triblock copolymer. Ten milligrams of **PHOS-FOL-DOX** polymer was dissolved in methanol. To this, 10 mg of magnetic nanoparticles (**Fe_3O_4**) was added and sonicated for 1 h. Excess polymer was washed out with methanol by magnetic filtration. In the process, 8 mg (80% yields) of black red color polymer obtained. IR (KBr, cm^{-1}): 3366, 2926, 2854, 1643, 1578, 1448, 1019, 772.

RESULTS AND DISCUSSION

Toward this goal, monomers, namely, cis-5-norbornene-6-(diethoxyphosphoryl)hexanote (**mono 1**), norbornene grafted poly(ethyleneglycol)-folate (**mono 2**), and norbornene derived doxorubicin (**mono 3**) were synthesized (SI Scheme S2). The complete characterization of these monomers are shown in Figure 1 and SI Figures S1−S17. The synthetic importance of the design was strongly encouraged by the freely water-soluble nature of **mono 2** (SI Scheme S2). Due to this, we envisioned that there would not be a need for separate PEG polymer segment to make the system water-soluble. It was suggested that polymerization of **mono 1** was done in a very controlled fashion. A series of **HP-PHO** of **mono 1**, **mono 2**, **HP-FOL**, **mono 3**, and **HP-DOX** (SI Scheme S3, SI Table 1) were made with different feed ratios ([M]/[I] = 10, 25, 40, 50) to evaluate the "livingness"

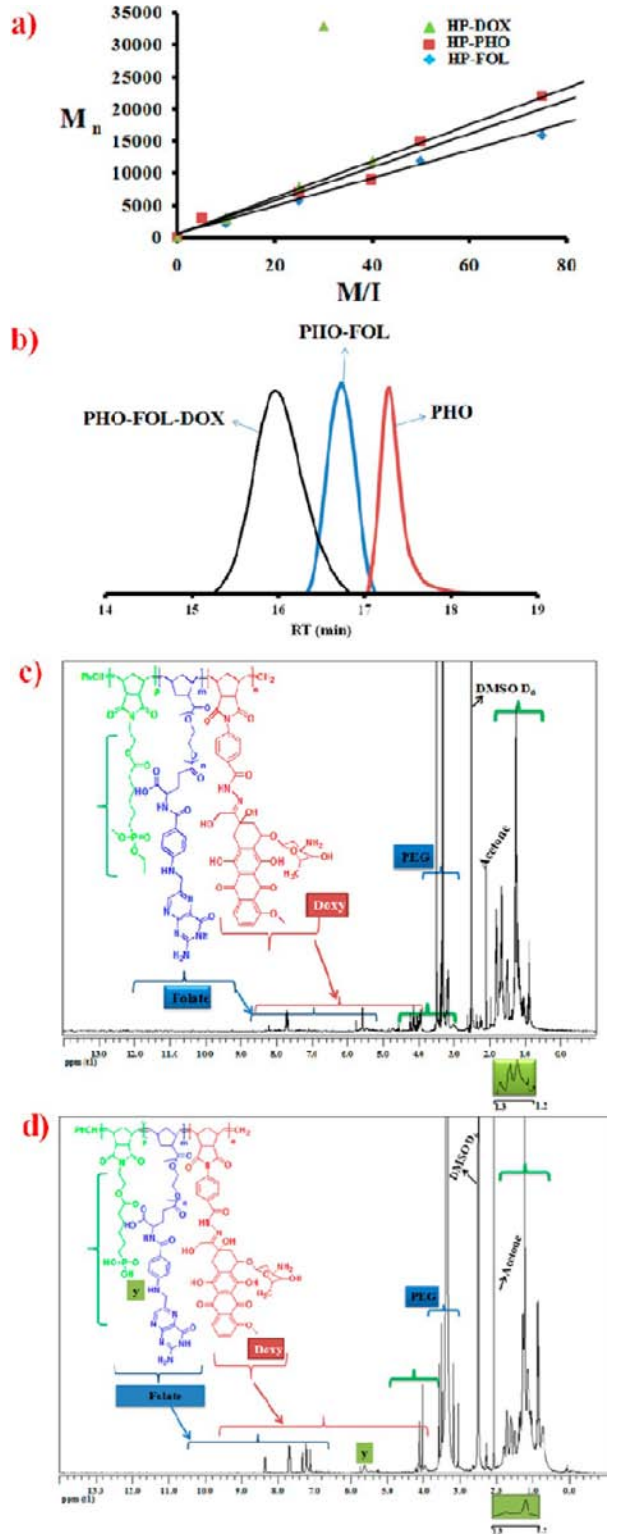

Figure 2. (a) "Livingness" of all homo polymers. (b) GPC analysis of triblock (**PHO-FOL-DOX**) copolymer (Mn = 33 kDa; PDI = 1.04), macroinitiator 2 (Mn 17 kDa; PDI = 1.1), macroinitiator 1 (Mn = 4 kDa; PDI = 1.1). (c) ^{1}H NMR spectrum of triblock copolymer (**PHO-FOL-DOX**). (d) ^{1}H NMR spectrum of triblock copolymer (**PHOS-FOL-DOX**).

of the polymerization (Figure 2a). It was observed that the polymerizations were well-controlled (SI Scheme S3, SI Table 1), resulting in narrow polydispersitiy index (PDI), with good

dx.doi.org/10.1021/bc400409n | Bioconjugate Chem. 2014, 25, 276−285

Table 1. GPC Results of PHOS-FOL-DOX

triblock copolymer	p[a]	m[b]	n[c]	p[d]	m[e]	n[f]	mol ratio[g] (p/m/n)	Mn,block th[h] (g/mol)	Mn, block (GPC)[i] (g/mol)	PDI[i]
PHO-FOL-DOX	15	15	15	10	8	20	0.1133	37000	33000	1.04

[a]Theoretical degree of polymerization (DP) of monomer **1**. [b]Theoretical DP of monomer **2**. [c]Theoretical DP of monomer **3**. [d]DP of monomer **1** by GPC. [e]DP of monomer **2** by GPC. [f]DP of monomer **3** by GPC. [g]Theoretical ratio of monomers in the triblock copolymer. [h]Theoretical number-average molecular weight (Mn). [i]Mn and polydisperisty index (PDI) were determined by GPC in THF relative to linear poly(methyl methacrylate) standards.

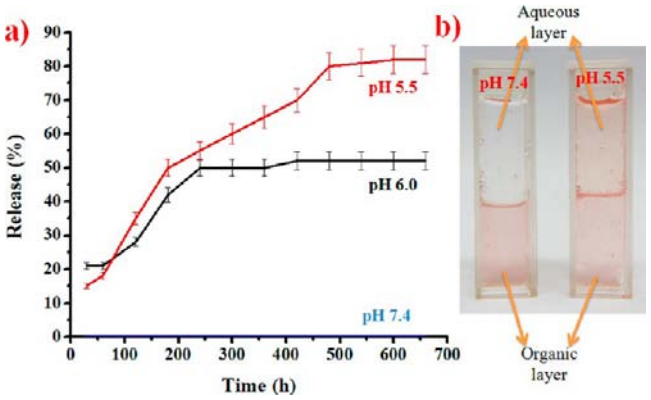

Figure 3. (a) DOX release profile of PHO-FOL-DOX micelles at 37 °C in comparison with pH 5.5, 6 and 7.4. (b) Pictorial representation of DOX release from of PHO-FOL-DOX at pH 5.5 and 7.4

yield (65−70%). Similarly, the homopolymerization of **mono 2**, **HP-FOL**, (SI Scheme S3, SI Table 1), homopolymer **HP-DOX**, and the results are shown in the SI Scheme S3 and SI Table 1.

After establishing the polymerization conditions for all the monomers, the triblock copolymerization (Scheme 1.) was carried out using second generation Grubbs' catalyst at room temperature in dry DCM and methanol (9:1 v/v %) solvent system by sequential addition of **mono 1**−**3**. The polymerization was monitored by ^{1}H NMR spectroscopy. The molecular weights of the macro initiator 1 (**PHO**, Mn = 4000, PDI = 1.1), macro initiator 2 (**PHO-FOL**, Mn = 17 000, PDI = 1.1), and the final triblock copolymer (**PHO-FOL-DOX**, Mn = 33 000, PDI = 1.05) were measured in GPC using polystyrene standards. The shifting of GPC traces in Figure 2b and Table 1 clearly indicated the formation of triblock copolymer, **PHO-FOL-DOX**. Also, the formation of **PHO-FOL-DOX** was confirmed through ^{1}H NMR and FTIR spectroscopy (Figure 2c). Before attaching the magnetic particles to the triblock copolymer, the in vitro drug release studies were carried out to test the stimuli responsive nature of the newly designed nanocarriers. For the drug release profile of **PHO-FOL-DOX**, pH 7.4 as well as acidic conditions were chosen to show the importance of hydrazone linker. Therefore, drug release study of **PHO-FOL-DOX** micelles was carried out in pH 7.4, 5.5, and 6.0 in phosphate buffer solutions, respectively (Figure 3a,b). For dialysis study, see SI for experimental procedure. The DOX release from **PHO-FOL-DOX** at pH 7.4 was minimal (less than 5%), which was very interesting to observe as it clearly demonstrated the **PHO-FOL-DOX** micelle's stability in the physiological condition. It was also worthy to note that the maximum as well as fast release was observed at pH 5.5 (80% of drug was released, Figure 3a) compared to pH 6 or pH 7.4 suggested the importance of having the acid-labile hydrazone linker in the **PHO-FOL-DOX**.

Magnetic Particle Attachment. For maximized therapeutic efficacy, nanocarrier-based cancer therapy should have minimum or no cargo leakage before reaching the target and controlled size

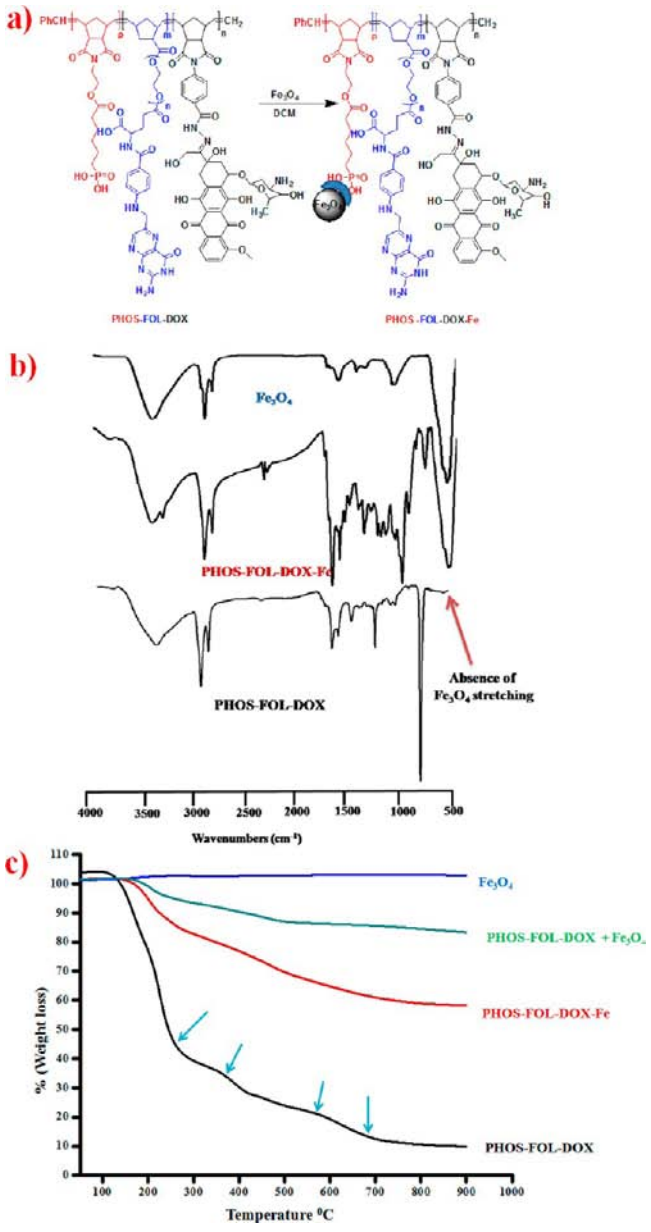

Figure 4. (a) Synthesis of PHOS-FOL-DOX-Fe. (b) FT-IR spectra of Iron nano particles (Fe3O4), PHO-FOL-DOX and PHOS-FOL-DOX-Fe (c) TGA data of PHOS-FOL-DOX triblock copolymer, PHOS-FOL-DOX-Fe, PHOS-FOL-DOX+Fe3O4 and Iron nano particles.

for effective extravasations.[21] Suppose the magnetic nanoparticles encapsulated into micelle (via nonconjugate approach) escape from the micelle before reaching the cancer site; they are likely to induce nanotoxicity, due to their very reactive surface area.[22−24] These particles also have a greater ability for translocation across biological membranes, or agglomeration, which can block blood vessels.[24,25] Due to this, unwanted accumulation

dx.doi.org/10.1021/bc400409n | Bioconjugate Chem. 2014, 25, 276−285

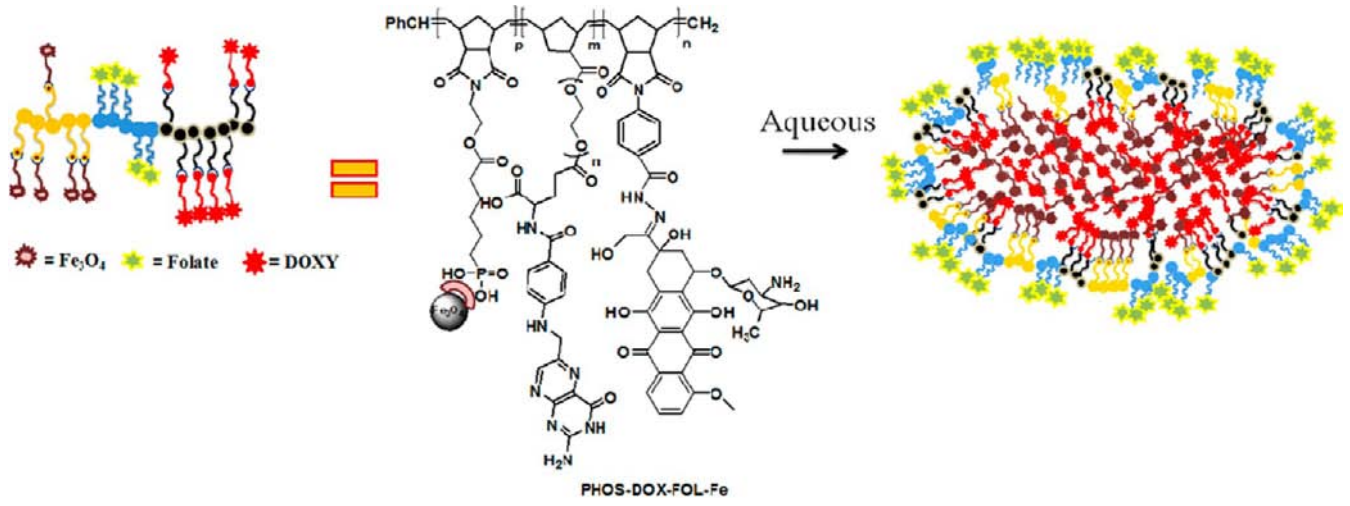

Figure 5. Cartoon representation for self-assembly of **PHOS-DOX-FOL-Fe**.

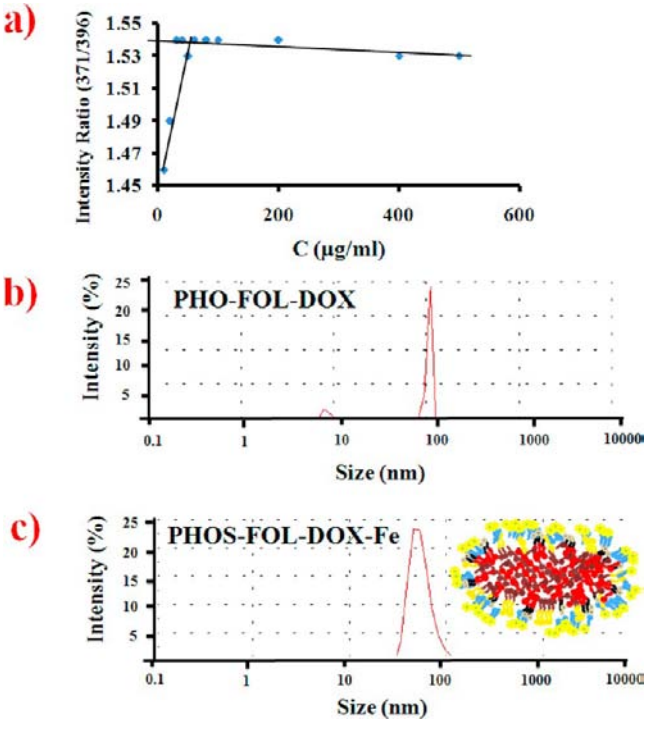

Figure 6. (a) CMC analysis of **PHO-FOL-DOX** (50 μg/mL) in methanol. (b) DLS analysis of **PHO-FOL-DOX** in methanol. (c) DLS analysis of **PHOS-FOL-DOX-Fe** in methanol.

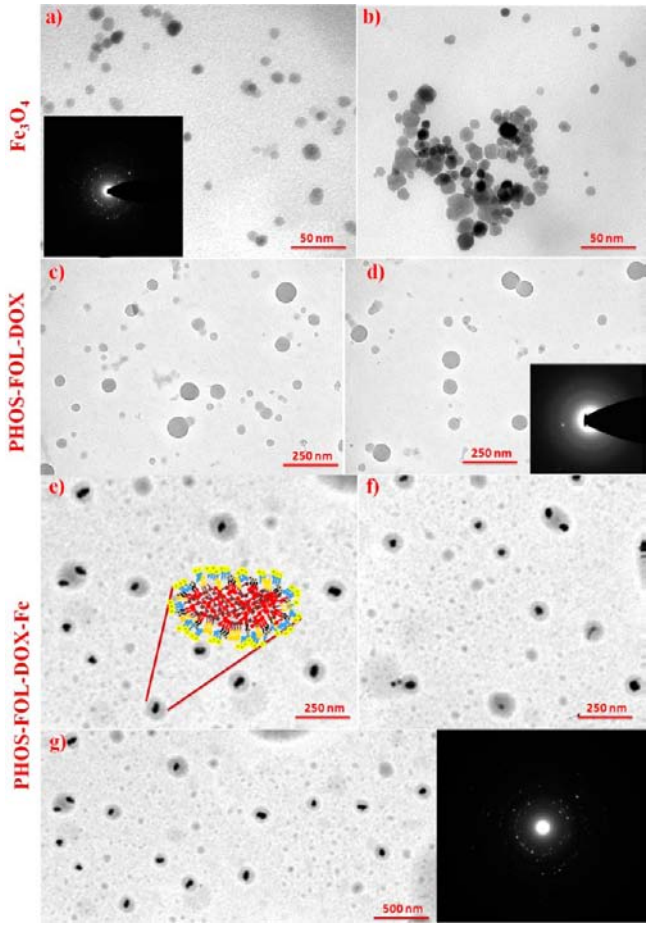

Figure 7. (a,b) TEM images of Fe_3O_4 nanoparticles; inset – SAED pattern of the Fe_3O4 nanoparticles; (c,d) TEM images of **PHOS-FOL-DOX**; inset – SAED of polymer; (e) and (g) TEM images of **PHOS-FOL-DOX-Fe**; inset – SAED pattern of the nano carrier.

of these particles in nontarget organs leads to huge side effects.[24] To overcome these physiological barriers in the body, a rational design of magnetic nanoparticles with controllable physicochemical properties and functional groups for bioconjugation is essential in the cancer research.[26−29] Toward this objective, **PHO-FOL-DOX** was successfully synthesized. Before the Fe_3O_4 conjugation, **PHO-FOL-DOX** was deprotected to get the phosphonic acid functionality to have a maximum attachment of the magnetic nanoparticles. Deprotection of phosphonate ester in **PHO-FOL-DOX** (SI Figure S18a) was carried by using trimethylsilyl bromide. The deprotection was confirmed by the ^{1}H NMR, FTIR, measurements. The signal at 1.2−1.3 ppm was absent in the deprotected triblock copolymer, **PHOS-FOL-DOX**, (Figure 2d) which indicated the product formation. The disappearance of the characteristic IR band at 1241 cm^{-1} supported the complete cleavage of phosphonate ester (SI Figure S18b).

After the successful deprotection, Fe_3O_4 nanoparticles conjugation was carried out. Magnetic nanoparticles were prepared by following the literature procedure.[36−39] Freshly synthesized

dx.doi.org/10.1021/bc400409n | *Bioconjugate Chem.* 2014, 25, 276−285

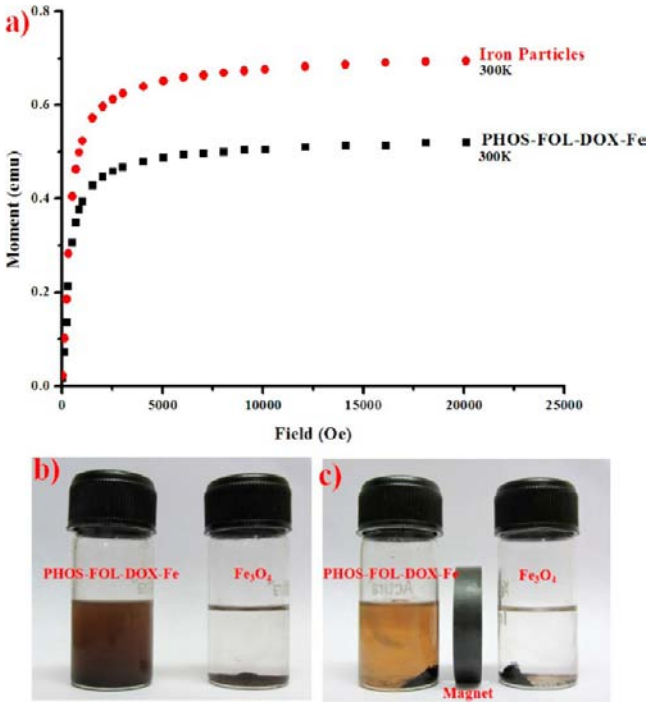

Figure 8. (a) Magnetic hysteresis loops of Fe_3O_4 and **PHOS-DOX-FOL-Fe**. (b,c) Manipulation by permanent magnet of Fe_3O_4 and **PHOS-DOX-FOL-Fe**.

Fe_3O_4 nanoparticles were functionalized with the **PHOS-FOL-DOX** triblock copolymer (Figure 4a). The appearance of the characteristic IR band at 1270, 1009 cm^{-1} corresponds to P═O bond, and the P−O bond along with the characteristic Fe_3O_4 band at 543 cm^{-1} (Figure 4b) confirmed the product formation of Fe_3O_4 particles attached triblock copolymer, **PHOS-FOL-DOX-Fe**. Thermogravimetric analysis (TGA) on **PHOS-FOL-DOX-Fe** also confirmed the conjugation of magnetic particle to the triblock copolymer. To prove that, first TGA of Fe_3O_4 alone was performed where there was no thermal degradation up to 800 °C. Similarly, TGA of **PHOS-FOL-DOX** alone was performed. It was observed that the triblock copolymer was stable up to 160 °C after which its first degradation point started. The polymer lost about 60 % of its weight before it reached the temperature 280 °C where the second degradation point started. The remaining 30% of the polymer's weight got degraded at the temperatures between 350 and 560 °C after which all the polymer completely degraded. Then. the TGA was performed on Fe_3O_4 conjugated triblock copolymer, **PHOS-FOL-DOX-Fe**. It was observed that **PHOS-FOL-DOX-Fe** was stable up to 220 °C which was about 60 °C higher than **PHOS-FOL-DOX**. We attributed this increment in the initial degradation temperature to the conjugation of particles to the OH motifs of phosphonic acid functionalities in **PHOS-FOL-DOX**. In an unbound state, the OH motifs got eliminated first at 160 °C, but due to the conjugation with Fe_3O_4 particles, they got little extended thermal stability up to 220 °C. This proposal was confirmed by a control experiment. TGA was performed on just a physical mixture of Fe_3O_4 particles and **PHOS-FOL-DOX** where the initial degradation point of the physical mixture was also observed at 160 °C. This was because the Fe_3O_4 was not conjugated, so polymer got degraded to its original first degradation point. All the other degradation pattern of **PHOS-FOL-DOX-Fe** were similar to that of **PHOS-FOL-DOX**. From the final weight of the

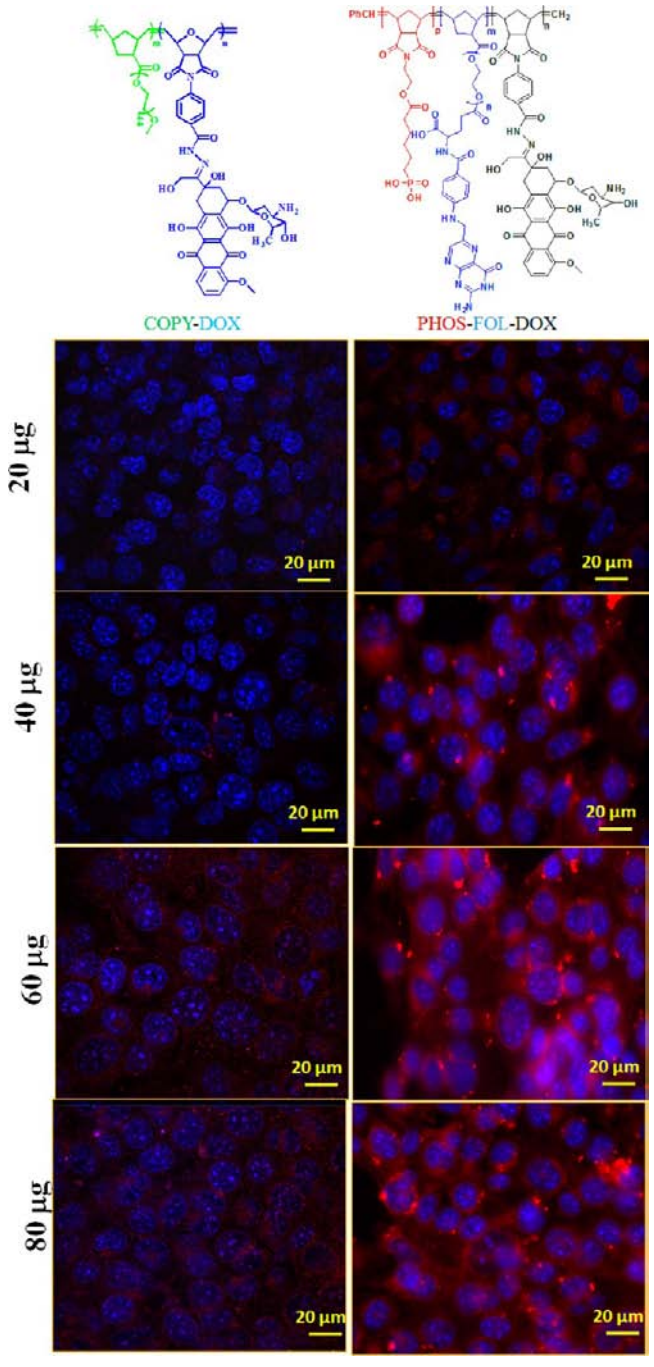

Figure 9. Confocal laser scanning microscope (CLSM) images of **COPY-DOX** as well as **PHOS-FOL-DOX** treated 4T cells.

degraded material, it was calculated that the amount of Fe_3O_4 particles conjugated to the polymer was about 45% (Figure 4c).

After confirming the conjugation of the magnetic particles to the block copolymer, we wanted to check the morphology of the particle attached nanocarrier, **PHOS-FOL-DOX-Fe** (Figure 5). The CMC of **PHOS-FOL-DOX** copolymer was measured by following a well-established method using pyrene as an extrinsic probe.[40] The observed CMC was 50 μg/mL (Figure 6a). Dynamic light scattering (DLS) analysis was performed in the solution that was used to measure the CMC. The size of the micelles was measured as 90 nm with 0.25 PDI (Figure 6b). The morphology of the micelles was determined by TEM (Figure7c). The observed spherical morphology with the diameter of about

dx.doi.org/10.1021/bc400409n | *Bioconjugate Chem.* 2014, 25, 276−285

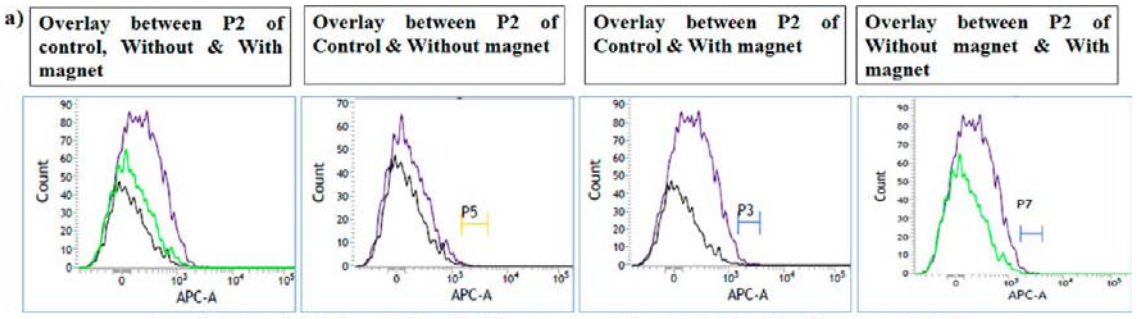

P2 of 'Control'- in **black**; P2 of 'Without magnet'- in **green**; P2 of 'With magnet'- in **blue**.

Name of the Tube	Events	Parent(%)	Grandparent (%)	Total (%)	FSC-A Mean	SSC-A Mean	APC-A Mean	APC-A SD	APC-A CV
Control: P3	4	0.18	0.04	0.04	35,770	89,190	1,740	183.15	10.52
With Magnet:P3	45	0.81	0.45	0.45	32,611	74,024	1,990	532.98	26.79
Control: P5	4	0.18	0.04	0.04	35,770	89,190	1,740	183,15	7.51
Without Magnet: P5	11	0.35	0.11	0.11	24,080	69,119	1,900	500.04	13.18
Without Magnet:P7	5	0.16	0.05	0.05	27,421	62,591	2,282	534.52	23.43
With Magnet: P7	31	0.58	0.31	0.31	32,327	78,057	2,177	546.73	25.11

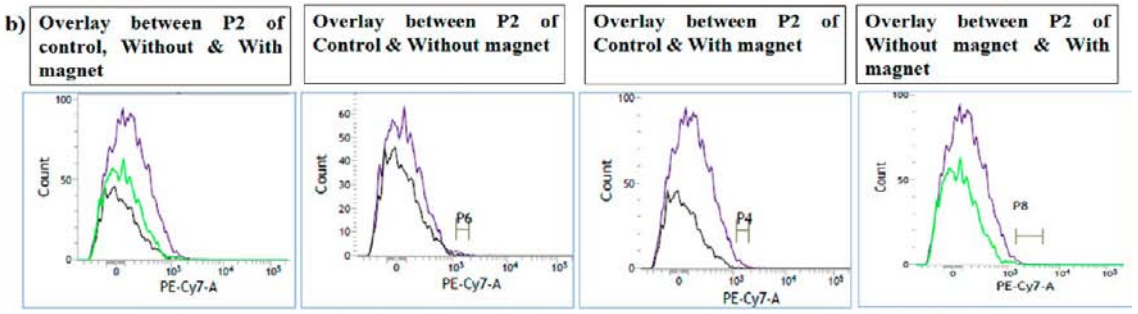

P2 of 'Control'- in **black**; P2 of 'Without magnet'- in **green**; P2 of 'With magnet'- in **blue**.

Name of the Tube	Events	Parent (%)	Grandparent (%)	Total (%)	FSC-A Mean	SSC-A Mean	PE-Cy7-A Mean	PE-Cy7-A SD	PE-Cy7-A CV
Control: P4	4	0.18	0.04	0.04	28,187	113,533	1,333	93,16	6.99
With Magnet:P4	45	0.81	0.45	0.45	27,516	77,496	1,421	170.14	11.97
Control: P6	4	0.18	0.04	0.04	28,187	113,533	1,333	93.16	6.99
Without Magnet: P6	18	0.57	0.18	0.18	25,952	81,511	1,413	200.47	14.19
Without Magnet:P8	6	0.19	0.06	0.06	24,268	80,722	1,736	234.16	13.49
With Magnet: P8	27	0.49	0.27	0.27	28,141	78,029	2,144	725.58	33.84

Figure 10. Flow cytometry analysis of (a) APC-A channel; (b) PECy7-A channel.

80−100 nm was in good agreement with the DLS observation. Similarly, the observed CMC of **PHOS-FOL-DOX-Fe** (Figure S19) was 300 μg/mL. From the DLS experiments (Figure 6c), it was interesting to observe that the nanocarrier's size slightly increased to about 130 nm from 90 nm after the conjugation with magnetic particles. This encouraged us to propose the following model for the nanocarrier. It advocates that under the aqueous and physiological environment, the nanocarrier would have relatively polar **FOL** motifs externally whereas internally it would have a hydrophobic drug part along with magnetic particle. This proposed model was strongly supported by the TEM experiments. From TEM analysis, the particle size was also measured at about 130 nm which was in good agreement with DLS measurements (Figure 7e and f). The selected area electron diffraction (SAED) pattern (inset in Figure 7a and b) indicated that the observed crystalline pattern was expected for magnetite particles.[41] TEM images of nanocarrier from **PHOS-FOL-DOX-Fe** copolymer suggested uniform shape and size. The observed increase in size of nanocarrier was mainly due to the magnetic nanoparticle conjugation. The SAED pattern of these nanocarriers showed no difference from that of magnetic particles alone (inset in Figure 7g), indicating that the conjugated nanoparticle did not change crystalline structure during the conjugation process. Obviously, it was not surprising that the SAED did not show any crystalline pattern for **PHOS-FOL-DOX** alone (inset in Figure 7d). Also, the TEM images with very dark core supported our proposed model of nanocarrier with DOX, Fe_3O_4 particle core, and folate corona.

The magnetic properties of Fe_3O_4 nanoparticles and **PHOS-FOL-DOX-Fe** nanocarriers were measured by magnetic property measurement system (MPMS) magnetometry at 300 K. A typical magnetization (M) vs applied magnetic field (H) curve at 300 K is shown in Figure8a. The recorded saturation magnetization for the nanocarrier was 50 emu/g, while for Fe_3O_4 particles alone, it was recorded as 65 emu/g. The observed

dx.doi.org/10.1021/bc400409n | *Bioconjugate Chem.* 2014, 25, 276−285

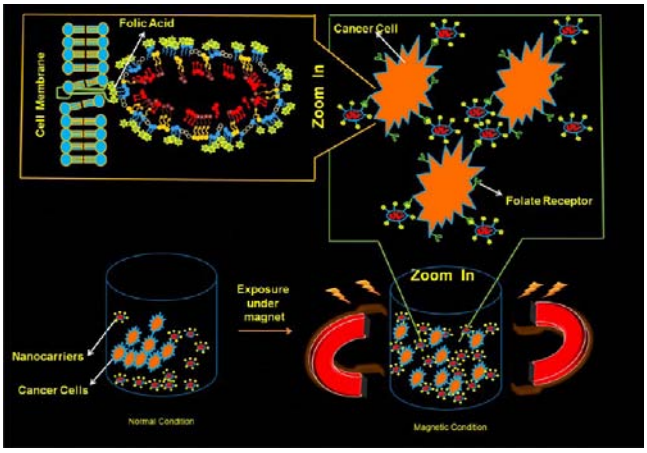

Figure 11. A cartoon representation of the magnetic field induced as well as receptor-mediated endocytosis of **PHOS-FOL-DOX-Fe** nanocarriers.

50 emu/g was considered to be a fairly high value for this type of hybrid multifunctional nanostructure.[42] We attributed this high magnetic strength from the nanocarrier to the close proximity and interaction of the magnetic particles conjugated in the triblock copolymer. Due to this, magnetostatic pull force could be expected in a gradient magnetic field. To test it quickly, the nanocarriers in aqueous solution were introduced to the permanent magnet. It was observed that the nanocarriers moved well in an aqueous solution toward the permanent magnet as shown in Figure 8b,c. We envisioned that this powerful magnetic vector of the nanocarriers would be effectively utilized for enhanced tumor penetration.

Receptor-Mediated Delivery. To demonstrate the specific cell uptake through receptor-mediated endocytosis of the newly designed nanocarriers, the 4T cells were observed by the confocal laser scanning microscope (CLSM) and the results are illustrated in Figure 9. The cellular uptake of **COPY-DOX**[19] and **PHOS-FOL-DOX-Fe** with increasing concentrations was studied by their intracellular distribution using confocal laser scanning microscope (Zeiss, LSM 710). The **COPY-DOX** was chosen as control molecule since it did not have any receptor molecule in the design. **FOL** motif in the nanocarrier was effectively received at the surface of the cancer cell due to the overexpressed folate receptor.

Next, to prove the magnetic field induced drug delivery, **PHOS-FOL-DOX-Fe** accumulated 4T cells were analyzed using flow cytometry (Figure 10). To prove that, three different experimental conditions were used: (i) 4T cells in suspension as control (no drug and no magnetic field), (ii) 4T cells in suspension with nanocarrier (no magnetic field), and (iii) 4T cells in suspension with nanocarrier were taken in MACS magnetic

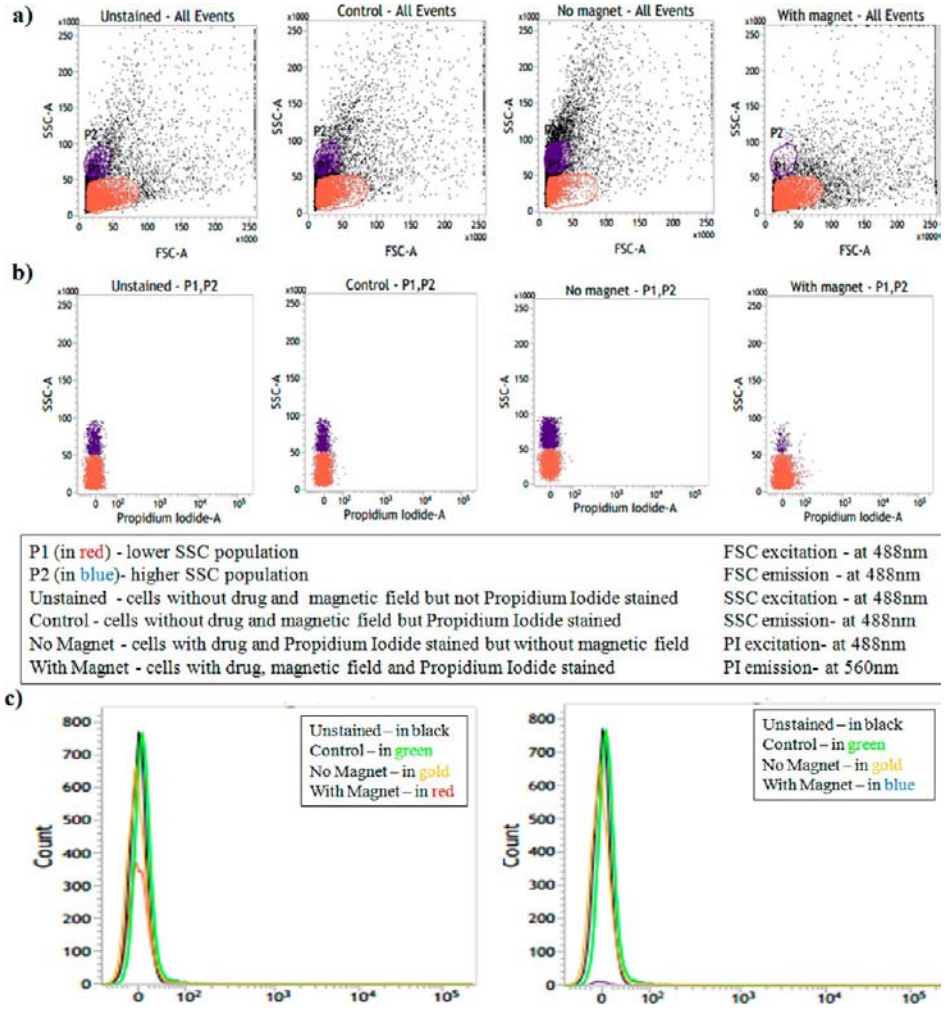

Figure 12. Cell viability data from flow cytometry analysis using propidium iodide.

dx.doi.org/10.1021/bc400409n | *Bioconjugate Chem.* 2014, 25, 276−285

column (Miltenyi Biotec) and kept in the presence of magnetic field as shown in Figure 11. To eliminate dead cells from living cell population, FSC (Forward Scatter Channel) vs SSC (Side Scatter Channel) were plotted. FSC was responsible for the cell size whereas SSC was for the cellular granularity. Since the nanocarrier could produce florescence emission in red spectrum due to DOX, two florescence channels, namely, APC (Allophycocyanin; Ex 640 nm, Em 660 nm) and PE-Cy7 (phycoerythrin-Cy7; Ex 488 nm, Em 752 nm) were chosen. The results were compared and tabulated in Figure 10. It was found that 0.58% (gate − P7) and 0.49% (gate − P8) of cells 'with magnet' exerted a clear intensity shift over cells 'without magnet' in both APC and PE-Cy7 channels, respectively. It was very interesting to note that the internalization of the nanocarrier was about 8 times greater in the presence of magnetic field compared to the condition without magnetic field. This observation was clinically very important because it could decrease the dosages of DOX and potentially overcome the drug resistance in cancer chemotherapy.

Influence of Magnetic Field. Finally, for cell viability assay, 1×10^5 cells were incubated with 50 μg/mL propidium iodide solution (BD) in the flow tube. It was clearly observed that only living cell populations were being dealt with (Figure 12a,b). No intensity shift on PI-A ('A' stands for area under the peak of propidium iodide intensity) axis was detected in the case of both higher and lower SSC population (Figure 12c). To best of our knowledge, this report clearly demonstrated the receptor-mediated along with magnetic field assisted efficient drug delivery.

CONCLUSION

In conclusion, norbornene based triblock copolymers conjugated with magnetic nanoparticles and anticancer drugs have been prepared using ROMP technique. The nanocarrier of the newly designed copolymer provides a powerful magnetic moment under moderate gradient magnetic fields. This smart nanocarrier is compact enough to meet the size requirement for a drug cargo, as all the components can be self-contained within 130 nm itself. Based on its distinct response to mild pH, combined with good magnetic response and folate motifs, this smart nanocarrier can serve as multiresponsive drug cargo. **PHOS-FOL-DOX-Fe** is the first nanocarrier to integrate targeting, pH-responsive, and magnetic field induced drug delivery for use in breast cancer research. Our unique design can open up a new avenue for a more effective cancer therapy through well-informed decision making. Detailed in vivo experiments on the newly developed system will be in a future report.

ASSOCIATED CONTENT

Supporting Information

Synthesis of monomer 3, homopolymers of all monomers, ^{1}H NMR, ^{13}C NMR, and IR spectra of monomers, dialysis study process. This material is available free of charge via the Internet at http://pubs.acs.org.

AUTHOR INFORMATION

Corresponding Author

*E-mail: sraja@iiserkol.ac.in.

Notes

The authors declare no competing financial interest.

ACKNOWLEDGMENTS

N.V.K. thank CSIR for the research fellowship. G.M.N. thanks UGC, New Delhi, for research fellowship. S.S. thank CSIR, New Delhi, for research fellowship. H.D., K.C., and T.D. thank DST. R.S. thanks Department of Science and Technology, New Delhi, for Ramanujan Fellowship and DBT for funding. R.S. and J.D.S. thank IISER-Kolkata for providing the infrastructure and startup funding. All the authors thanks Dr. Chiranjib Mitra and Mr. Harkirat Singh, Department of Physical Science, IISER-Kolkata, for the MPMS magnetometry measurements.

REFERENCES

(1) Duncan, R. (2006) Polymer conjugates as anticancer nanomedicines. *Nat. Rev. Cancer 6*, 688−701.
(2) Duncan, R. (2003) The dawning era of polymer therapeutics. *Nat. Rev. Drug Discovery 2*, 347−360.
(3) Yang, X., Chen, Y., Yuan, R., Chen, G., Blanco, E., Gao, J., and Shuai, X. (2008) Folate encoded and Fe_3O_4-loaded polymeric micelles for dual targeting of cancer cells. *Polymer 49*, 3477−3485.
(4) Hong, G. B., Yuan, R. X., Liang, B. L., Shen, J., Yang, X. Q., and Shuai, X. (2008) Folate functionalized polymeric micelle as hepatic carcinoma-targeted, MRI-ultrasensitive delivery system of antitumor drugs. *Biomed. Microdevices 10*, 693−700.
(5) Dong, H., Dube, N., Shu, J. Y., Seo, J. W., Mahakian, L. M., Ferrara, K. W., and Xu, T. (2012) Long-circulating 15 nm micelles based on amphiphilic 3-helix peptide-PEG conjugates. *ACS Nano 6*, 5320−5329.
(6) Shu, J. Y., Tan, C., DeGrado, W. F., and Xu, T. (2008) New design of helix bundle peptide-polymer conjugates. *Biomacromolecules 9*, 2111−2117.
(7) Zebli, B., Susha, A. S., Sukhorukov, G. B., Rogach, A. L., and Parak, W. J. (2005) Magnetic targeting and cellular uptake of polymer microcapsules simultaneously functionalized with magnetic and luminescent nanocrystals. *Langmuir 21*, 4262−4265.
(8) Yin, Y., Rioux, R. M., Erdonmez, C. K., Hughes, S., Somorjai, G. A., and Alivisatos, A. (2004) Formation of hollow nanocrystals through the nanoscale Kirkendall effect. *Science 304*, 711−714.
(9) Gillies, E. R., and Frechet, J. M. J. (2005) pH-Responsive copolymer assemblies for controlled release of doxorubicin. *Bioconjugate Chem. 16*, 361−368.
(10) Gillies, E. R., and Frechet, J. M. J. (2003) A new approach towards acid sensitive copolymer micelles for drug delivery. *Chem. Commun. 14*, 1640−1641.
(11) Lehn, J.-M., and Eliseev, A. (2001) Dynamic combinatorial chemistry. *Science 291*, 2331−2332.
(12) Gillies, E. R., and Frechet, J. M. J. (2004) Development of acid-sensitive copolymer micelles for drug delivery. *Pure Appl. Chem. 76*, 1295−1307.
(13) Bae, Y., Fukushima, S., Harada, A., and Kataoka, K. (2003) Design of environment-sensitive supramolecular assemblies for intracellular drug delivery: polymeric micelles that are responsive to intracellular pH change. *Angew. Chem., Int. Ed. 42*, 4640−4643.
(14) Grubbs, R. H. *Handbook of Metathesis*; Wiley-VCH: New York, 2003; Vol 3.
(15) Watson, K. J., Park, S.-J., Im, J.-H., and Nguyen, S. T. (2001) Toward polymeric anticancer drug cocktails from ring-opening metathesis polymerization. *Macromolecules 34*, 3507−3509.
(16) Sheldon, Y. O., and Grubbs, R. H. (2000) Synthesis of norbornenyl polymers with bioactive oligopeptides by ring-opening metathesis polymerization. *Macromolecules 33*, 6239−6248.
(17) Pollino, J. M., Stubbs, L. P., and Weck, M. (2003) Living ROMP of exo-norbornene esters possessing PdII SCS pincer complexes or diaminopyridines. *Macromolecules 36*, 2230−2234.
(18) Rao, V. N., Kishore, A., Sarkar, S., Das Sarma, J., and Shunmugam, R. (2012) Norbornene-derived poly-D-lysine copolymers as quantum dot carriers for neuron growth. *Biomacromolecules 13*, 2933−2944.
(19) Rao, V. N., Mane, S. R., Kishore, A., Das Sarma, J., and Shunmugam, R. (2012) Norbornene derived doxorubicin copolymers as

drug carriers with pH responsive hydrazone linker. *Biomacromolecules 13*, 221−230.
(20) Mane, S. R., Rao, V. N., Chatterjee, K., Dinda, H., Nag, S., Kishore, A., Das Sarma, J., and Shunmugam, R. (2012) Amphiphilic homopolymer vesicles as unique nano-carriers for cancer therapy. *Macromolecules 45*, 8037−8042.
(21) Dong, H., Dube, N., Shu, J. Y., Seo, J. W., Mahakian, L. M., Ferrara, K. W., and Xu, T. (2012) Long-circulating 15 nm micelles based on amphiphilic 3-helix peptide PEG conjugates. *ACS Nano 6*, 5320−5329.
(22) Moghimi, S. M., hunter, A. C., and Murray, J. C. (2001) Long-circulating and target-specific nanoparticles: theory to practice. *Pharmacol. Rev. 53*, 283−318.
(23) Kim, E., Lee, K., Huh, Y. M., and Haam, S. (2013) Magnetic nano complexes and the physiological challenges associated with their use for cancer imaging and therapy. *J. Mater. Chem. B. 1*, 729−739.
(24) Nel, A., Xia, T., Madler, L., and Li, M. (2006) Toxic potential of materials at the nanolevel. *Science 311*, 622−627.
(25) Kim, E., Lee, K., Huh, Y. M., and Haam, S. (2013) Magnetic nanocomplexes and the physiological challenges associated with their use for cancer imaging and therapy. *J. Mater. Chem. B. 1*, 729−739.
(26) Yoo, D., Lee, J. H., Shin, T. H., and Cheon, J. (2011) Theranostic magnetic nanoparticles. *Acc. Chem. Res. 44*, 863−874.
(27) Ho, D., Sun, X., and Sun, S. (2011) Monodisperse magnetic nanoparticles for theranostic applications. *Acc. Chem. Res. 44*, 875−882.
(28) Bilalis, P., Chatzipavlidis, A., Tziveleka, L. A., Boukosa, N., and Kordas, G. (2012) Nanodesigned magnetic polymer containers for dual stimuli actuated drug controlled release and magnetic hyperthermia mediation. *J. Mater. Chem. 22*, 13451−13454.
(29) Ma, W. F., Wu, K. Y., Tang, J., Li, D., Wei, C., Guo, J., Wang, S. L., and Wang, C. C. (2012) Magnetic drug carrier with a smart pH-responsive polymer network shell for controlled delivery of doxorubicin. *J. Mater. Chem. 22*, 15206−15214.
(30) Kim, B. S., Qiu, J. M., Wang, J. P., and Taton, T. A. (2005) Magneto micelles: Composite nanostructures from magnetic nanoparticles and cross-linked amphiphilic block copolymers. *Nano Lett. 5*, 1987−1991.
(31) Herdt, A. R., Kim, B.-S., and Taton, T. A. (2007) Encapsulated magnetic nanoparticles as supports for proteins and recyclable biocatalysts. *Bioconjugate Chem. 18*, 183−189.
(32) Kim, J., Lee, J. E., Lee, S. H., Yu, J. H., Lee, J. H., Park, T. G., and Hyeon, T. (2008) Designed fabrication of a multi functional polymer nanomedical platform for simultaneous cancer-targeted imaging and magnetically guided drug delivery. *Adv. Mater. 20*, 478−83.
(33) Lee, H., Lee, E., Kim, D. K., Jang, N. K., Jeong, Y. Y., and Jon, S. (2006) Antibiofouling polymer-coated super paramagnetic iron oxide nanoparticles as potential magnetic resonance contrast agents for in vivo cancer imaging. *J. Am. Chem. Soc. 128*, 7383−7389.
(34) Yuan, J.-J., Armes, S. P., Takabayashi, Y., Prassides, K., Leite, C. A. P., Galembeck, F., and Lewis, A. L. (2006) Synthesis of biocompatible poly [2-(methacryloyloxy)ethyl phosphorylcholine]- coated magnetite nanoparticles. *Langmuir 22*, 10989−93.
(35) Fan, Q.-L., Neoh, K.-G., Kang, E.-T., Shuter, B., and Wang, S.-C. (2007) Solvent-free atom transfer radical polymerization for the preparation of poly (ethyleneglycol) monomethacrylate)- grafted Fe_3O_4 nanoparticles: synthesis, characterization and cellular uptake. *Biomaterials 28*, 5426−36.
(36) Yang, X., Chen, Y., Yuan, R., Chen, G., Blanco, E., Gao, J., and Shuai, X. (2008) Folate encoded and Fe_3O_4-loaded polymeric micelles for dual targeting of cancer cells. *Polymer 49*, 3477−3485.
(37) Hong, G. B., Yuan, R. X., Liang, B. L., Shen, J., Yang, X. Q., and Shuai, X. T. (2008) Folate functionalized polymeric micelle as hepatic carcinoma-targeted, MRI-ultrasensitive delivery system of antitumor drugs. *Biomed. Microdevices 10*, 693−700.
(38) Esmaeili, F., Ghahremani, M. H., Ostad, S. N., Atyabi, F., Seyedabadi, M., Malekshahi, M. R., Amini, M., and Dinarvand, R. (2008) Folate-receptor-targeted delivery of docetaxel nanoparticles prepared by PLGA-PEG-folate conjugate. *J. Drug Targeting 16*, 415−423.
(39) Licciardi, M., Giammona, G., Du, J. Z., Armes, S. P., Tang, Y. Q., and Lewis, A. L. (2006) New folate-functionalized biocompatible block copolymer micelles as potential anti-cancer drug delivery systems. *Polymer 47*, 2946−2955.
(40) Hyuk, S. Y., Lee, E. H., and Park, T. G. (2002) Doxorubicin-conjugated biodegradable polymeric micelles having acid-cleavable linkages. *J. Controlled Release 82*, 17−27.
(41) Yang, X., Chen, Y., Yuan, R., Chen, G., Blanco, E., Gao, J., and Shuai, X. (2008) Folate encoded and Fe_3O_4-loaded polymeric micelles for dual targeting of cancer cells. *Polymer 49*, 3477−3485.
(42) Dunn, S. S., Byrne, J. D., Perry, J. L., Chen, K., and Desimone, J. M. (2013) Generating Better medicines for cancer. *ACS Macro Lett. 2*, 393−397.